Multi-sensor Observations of the SpinSat Satellite

Doyle Hall[1], Paul Kervin[2], Andrew Nicholas[3], Jake Griffiths[3], Ivan Galysh[3], and Michael Werth[1]

[1]*Boeing LTS, Kihei, Maui, HI and Colorado Springs, CO*
[2]*Air Force Research Laboratory, Kihei, Maui, HI*
[3]*Naval Research Laboratory, Washington DC*

1   SUMMARY

The Naval Research Laboratory developed and launched the spherical SpinSat satellite to accomplish two primary goals: 1) study the performance of a new class of micro-thrusters, and 2) provide a calibrated drag experiment to characterize Earth's upper atmosphere during the current period of relatively high solar activity. The 55.9 cm diameter aluminum sphere is equipped with a set of Electrically-Controlled Solid Propellant (ESP) thrusters, oriented to allow both translational and spin-up/spin-down maneuvers. To facilitate remote observations of the satellite's spin rate, the sphere's exterior features a reflectance pattern much like that of a beach-ball, a distributed sequence of retro-reflectors, as well as an ensemble of eight light-emitting diodes (LEDs) arranged along a meridian (i.e., a line of longitude) which can be turned on for brief periods. The Air Force Research Laboratory has conducted optical observations of SpinSat from several Advanced Maui Optical and Space Surveillance (AMOS) observatory sensors. The observational goals include: 1) obtaining time-resolved, multi-band measurements of the satellite actively firing its micro-thrusters, 2) characterizing the detectability and spatial/temporal morphology of the ESP thruster plumes, 3) measuring the spin rate of the satellite with the LEDs turned on, ideally before and after a spin rate adjustment maneuver, and 4) measuring the spin rate of the satellite in its completely inactive mode, using only passive observations of reflected light and/or thermal emissions.

Three SpinSat terminator passes were observed using multiple AMOS sensors on 2015 April 02 and 04. These observations were preceded by three attempts to uplink a sequence of thruster-firing and LED on/off commands from SpinSat's ground-station. The first two uplinked command-loads were erased by the satellite resetting itself, likely caused by passage through the high-radiation environment of the South Atlantic Anomaly (SAA). SpinSat's status logs indicate no reset occurred after the third and final uplink. However, our analysis of the AMOS SpinSat light-curve data strongly suggests that a timing error of exactly one minute may have occurred during the third command-load uplink process. Based on this assumption, then our analysis of the data collected during the highest-quality AMOS pass indicates the following conclusions: 1) The ESP micro-thruster firing event caused a sudden brightening in the near-IR temporal radiometry light-curves of ~0.5 magnitude. 2) However, the spatial signature of ESP micro-thrusters and/or their associated plumes were not detected in the near-IR imagery, even using the AEOS telescope with an aperture diameter of 3.6 m. 3) The ESP thruster-firing and LED on/off events were also not detected in the AEOS 3.6m thermal-IR imagery nor the thermal-IR whole-object radiometry. 4) One of the LED on/off events caused a sudden near-IR change of brightness of ~0.8 magnitude near-IR, but two other such events were apparently obscured because SpinSat's line of LEDs happened to be oriented largely on the opposite side of the slowly spinning sphere than the observing sensor.

2   INTRODUCTION

The Naval Research Laboratory (NRL) has deployed several spherical satellites to characterize Earth's upper atmosphere among other auxiliary objectives. The SpinSat satellite [1] represents the latest in this series; it was deployed into low-Earth orbit (LEO) from the International Space Station (ISS) in late November of 2014, a few weeks after having been delivered by a SpaceX Dragon supply ship. The launch and deployment of SpinSat were supported by the DoD Space Test program. Figure 1 shows a pre-launch photograph of the 22-inch diameter SpinSat satellite, along with an exploded-view of its components.   The sphere's exterior features a reflectance pattern much like that of a beach-ball, a distributed sequence of retro-reflectors, as well as a set of eight light-emitting diodes (LEDs) arranged along a meridian (i.e., a line of longitude) which can be turned on for brief periods. In addition to atmospheric studies, the SpinSat mission aims to study the performance of a new class of micro-thrusters [1]. These Electrically-Controlled Solid Propellant (ESP) thrusters, developed by Digital Solid State Propulsion, are mounted in twelve clusters on the SpinSat body (see Figure 1), oriented to allow both translational and spin-up/spin-down maneuvers. Each cluster contains six individual ESP thruster units, and each unit extends ~13 mm in length into the spherical body and contains a total of ~0.1 g of propellant [1].

In early 2015, researchers at the Air Force Research Laboratory (AFRL) began collaboration with the NRL SpinSat team, with the goal of using multiple AMOS sensors to observe the satellite firing the ESP micro-thruster thrusters, and turning the LEDs on and off.
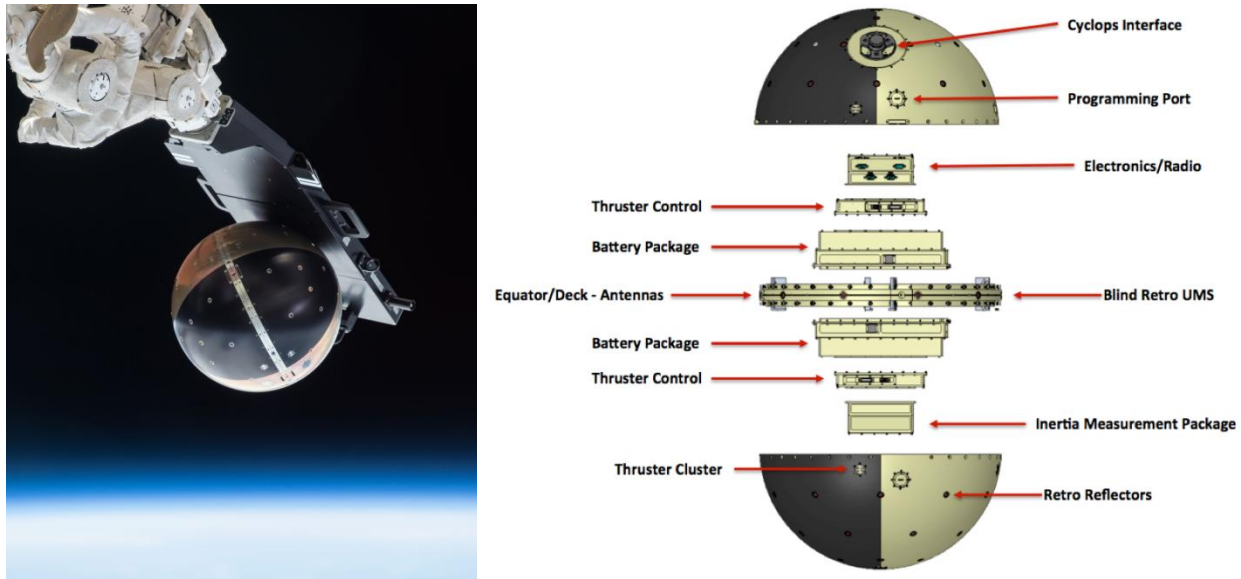

Figure 1. Photograph of SpinSat (left, courtesy NASA) mounted on the ISS mechanical arm before deployment, and an exploded-view of the internal and external components (right) of the 22-inch diameter spherical satellite [1].

3   OBSERVATION OF THE SPINSAT SATELLITE

3.1   Coordinated Passes for Uplink Telemetry and Optical Observations

Finding appropriate times to conduct the SpinSat observations represented a challenge because several scheduling constraints needed to be satisfied. First, the optical AMOS telescopes generally require "terminator passes" to observe LEO satellites such as SpinSat, i.e., traversals of the sunlit satellite over the non-sunlit observatory. To ensure good observation opportunities for the LED/thruster events, the team also required the AMOS passes to achieve an altitude angle (i.e., elevation) of at least 45°. Before the AMOS passes, SpinSat had to be commanded to perform the LED/thruster activities, which requires uplink telemetry from NRL's SpinSat ground-station located in the Chantilly, VA area. These command-load uplinks generally require ground-station passes culminating above elevations of 55°, although somewhat lower passes can sometimes suffice. Satisfying all of the scheduling constraints entails predicting when one or more AMOS terminator passes will be preceded by an appropriate set of SpinSat ground-station passes. Unfortunately, because of its low altitude orbit, SpinSat experiences significant atmospheric drag which can only be forecast to a limited accuracy, so the passes could only be predicted to sufficient accuracy for about three weeks into the future. In early 2015, the team began searching for appropriate combinations of passes for the two sites, performing pass-prediction calculations once every two weeks or so, projecting forward three-weeks in each case. In mid-March, the predictions indicated a suitable combination of three AMOS terminator passes on 2015 April 02 and 04 (see Figure 2 and Table 1) with several suitable SpinSat ground-station uplink passes occurring within the preceding 5 days (see Figure 3).

Ideally, the uplink passes would precede the command execution times by as few orbital revolutions as possible. The primary reason for this is that SpinSat occasionally resets (i.e., reboots itself) when subjected to unexpectedly high levels of environmental radiation, losing all of the commands contained within its buffer. After such a reset event, it will fail to perform any remaining, unexecuted commands. This radiation-induced reset risk can be minimized by choosing pass sequences that avoid known high-radiation environments when possible.   Unfortunately, the combined scheduling constraints discussed above produced a pass sequence accompanied traversals through the SAA region. So in this case, the reset risk can be minimized by reducing the time between command uplink and execution as much as possible, and closely monitoring the spacecraft's event-status log to detect any such reset events, allowing new command-load sequences to be uplinked as required.
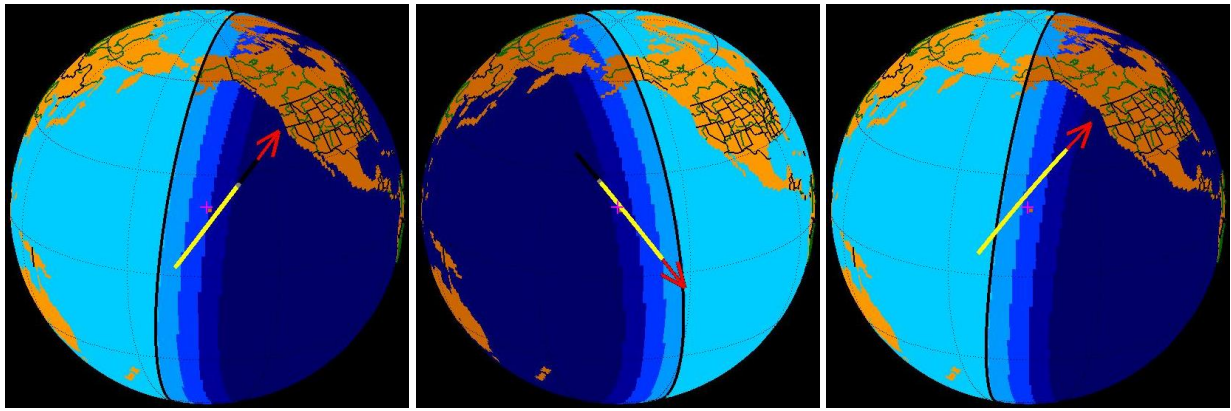
Figure 2. Ground-track plots showing the observational geometry of the three SpinSat passes observed from the AMOS observatory (see Table 1 for details). In each plot, the pink cross (+) shows the position of AMOS. The lines show the ground-track of SpinSat during the passes, with the red arrow indicating the direction of motion. The colors of the ground-tracks illustrate the solar illumination and Earth-shadow conditions as follows: yellow = fully sunlit, gray = penumbra, and black = umbra.

Table 1. Details of the three SpinSat passes observed from AMOS (as shown in Figure 2).

Pass Timing, Geometry and Object Illumination Details[a,b]			
Pass Number	1	2	3
Date	2015-04-02	2015-04-02	2015-04-04
Rise	05:21:18 - sunlit	15:08:45 - umbra	05:07:08 – sunlit
Culmination	05:26:28 - sunlit	15:13:58 - sunlit	05:12:20 - sunlit
(Max. El., Min. Range)	(44.7°, 547 km)	(81.6°, 394 km)	(51.5°, 496 km)
Set	05:31:38 - umbra	15:19:10 – sunlit	05:17:33 – sunlit
Nominal Estimated SpinSat Command Execution Times[c,d,e]			
LEDs ON	05:23:51	15:11:21	05:09:34
LEDs OFF	05:26:51	15:14:21	05:12:34
Thruster Firing[d]	05:27:06	15:14:36	05:12:49
LEDs ON	05:27:21	15:14:51	05:13:04
LEDs OFF	05:30:21	15:17:51	05:16:04
AMOS 3.6 m Telescope Sensors - Data Acquisition and Quality Summary[f]			
LAAT (ACQ-WFOV)	▲	▲	▬
DI (NFOV)	▲	▬	▬
ARDI (NFOV)	▬	▲	▬
LWIR (NFOV)	▶	▲	▬
AMOS 1.6 m Telescope Sensors - Data Acquisition and Quality Summary[f]			
AATS (ACQ-WFOV)	▲	▼	▲
Flash (NFOV)	▲	▼	▲

[a]All times specified in UTC.
[b]All pass parameters estimated using a two-line orbital element set for SCN 40314 with epoch 15092.86416163.
[c]All nominal LED and thruster firing command execution times are uncertain by approximately ± 2 s.
[d]Each ESP micro-thruster firing event had a duration of 0.2 s.
[e]There is some evidence that these events may have executed 1 minute earlier than these intended times.
[f]Collected data/signal quality key: ▲ = good, ▶ = marginal, ▼ = poor or none, ▬ = not attempted

3.2   Scheduled LED Activation/Deactivation and Thruster Firing Events

During the period of this study, SpinSat passes over any particular ground site lasted ~10 minutes from rise to set. Most telescopes cannot observe at very low elevation angles, and also need some time to acquire, track, and begin recording data, leaving only about six or seven minutes of usable observation time during each pass. Because of this, we designed the LED on/off and thruster firing events to span the central 6.5 minutes of each AMOS pass, intending the thruster to fire just a bit past the pass culmination point, i.e., just past the point of maximum elevation. The LEDs were to be activated early in the pass, in part to aid the acquisition and tracking of the object, and also to possibly facilitate spin rate measurements before firing the thruster. Table 2 shows this schedule of commanded

events, tabulated as a function of time relative to that of the pass culmination. The set of SpinSat thrusters commanded to fire at culmination + 15 s only included the "spin-up/spin-down" ESP-clusters (i.e., those devoted to modifying the satellite's spin rate rather than those for exerting translational force), and each firing lasted for 0.2 s.

Table 2. Nominal Pattern and Timing of SpinSat Commanded Events

Uplinked Command	Intended Time Relative to AMOS Pass Culmination (minutes)
LEDs ON	−3.00
LEDs OFF	−0.00
Thruster Firing	+0.25
LEDs OFF	+0.50
LEDs ON	+3.50

3.3 Uplink Telemetry Command Relative Timing

SpinSat's uplink telemetry entails transmitting to the spacecraft the times of the events to be executed by the spacecraft *measured relative to the time of the execution of the uplinked command-load*. For instance, in broad terms, an LED activation command might entail instructing SpinSat to "turn on the LEDs 99176 s after receiving this command-load sequence". This means that each command actually needs to be uplinked in association with a relative offset time, rather than an absolute time. These uplinked offset times need to account for three things: a) the desired time for the event measured relative to culmination as given in Table 2, b) the estimated pass culmination times as given in Table 1, and c) the time that the telemetry command-load was actually executed. This uplink command timing process is not automated, and therefore subject to human error when calculating and entering the offset times. Furthermore, even if all of the command offset times were processed by the ground-station operator correctly, the exact timing is still imprecise, primarily because of the uncertainty in estimating the actual uplink command-load reception times. Each uplinked command-load included instructions for SpinSat to execute the set of five LED/thruster events listed in Table 2 for all three of the AMOS passes. Table 1 provides the *nominal* times for these command execution events. However, there is some evidence in the AMOS light-curve data (discussed below) that these events actually occurred exactly *one minute earlier* than the intended nominal estimates. An error of such a round-number timing offset is not inconceivable, given the uplink command steps outlined above.
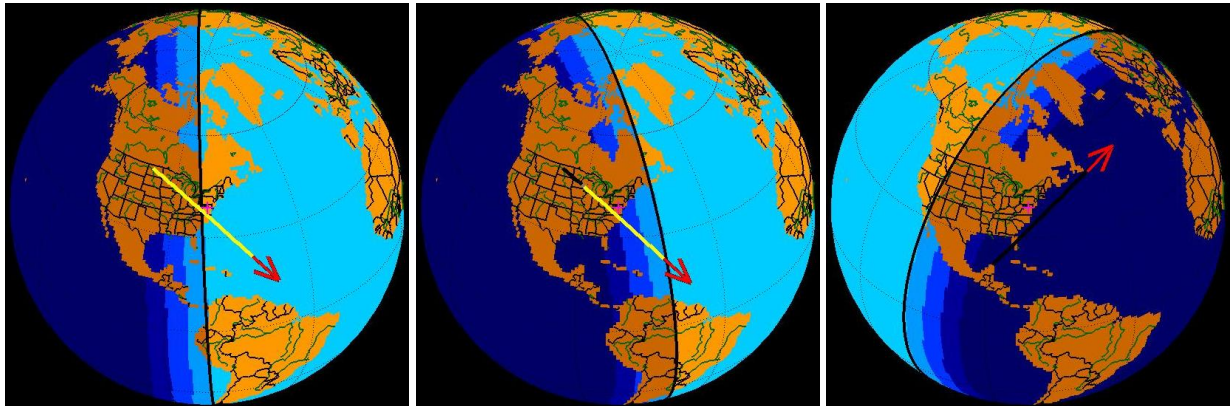

Figure 3. Ground-track plots of three of the passes used for command-load uplink telemetry by the SpinSat ground-station, located near Chantilly, VA. The earliest pass (left panel) occurred at 2015-03-27 0711-0721 EST. However, because of subsequent spacecraft resets, likely caused by elevated radiation levels encountered during SpinSat's traversals through the SAA, the command sequence had to be uplinked again during a second pass (middle panel) at 2015-03-30 0602-0612 EST, and a final third pass (right panel) at 2015-03-31 2144-2154 EST.

3.4 Spacecraft Reset Events Likely Caused by the South Atlantic Anomaly

The first command-load uplink occurred during a SpinSat pass above the Chantilly ground-station which occurred at 2015-03-27 1111-1121 UT (0711-0721 EST), shown on the left panel of Figure 3. However, a check of SpinSat's logged status conducted after the next ground-station overpass, several hours later, revealed the satellite had reset itself during the intervening period, likely because of elevated radiation levels encountered while traversing the SAA region of Earth's magnetosphere (discussed below). So the command sequence was uplinked again during a second pass, shown in the middle panel of Figure 3, at 2015-03-30 1002-1012 UT (0602-0612 EST). A subsequent check

of the status-log indicated that the spacecraft had again reset. So the commands were uploaded a third time during a night-time pass at 2015-04-01 0144-0154 UT (2015-03-31 2144-2154 EST), shown in the right panel of Figure 3.

The SpinSat reset events were likely caused by the spacecraft traversing the SAA, which is a region in Earth's magnetosphere where the inner Van Allen radiation belts dip in altitude and significantly elevate charged particle radiation levels (see [2] and references therein). The SAA lies roughly above the eastern tip and south-eastern coast of South America. Notably, the pass-geometry plots in Figure 3 show SpinSat headed for precisely that SAA region just after the first two uplink attempts (left and middle panels), which were the ones that suffered from subsequent reset events. No subsequent SpinSat reset events were detected after this third and final uplink pass, which preceded the first observed AMOS pass by ~27.5 hours.

The final estimates for the nominal SpinSat LED and thruster event execution times given in Table 1 are based on the ground-station's operator's best estimates for the timing of this final uplinked command-load. Each uplinked execution time has an estimated uncertainty of about ± 2 s. However, as mentioned previously, the AMOS data suggests that these events may have actually occurred exactly one minute earlier than these intended nominal estimates, which would be have been due to a systematic error of a different nature.

3.5   Summary of AMOS Observations

Multiple sensors from the AMOS observatory's 3.6m and 1.6m telescopes were used to observe the three passes shown in Figure 2. Table 1 includes color-coded summaries of the status and quality for the collected data sets. The sensors include two acquisition sensors (LAAT and AATS) which are small, side-mounted, co-aligned telescopes imaging visible-band emissions using silicon-based CCD detectors, each with a relatively wide field-of-view (WFOV) subtending ~30 arcmin.   The 3.6m and 1.6m telescopes also host one or more narrow field-of-view (NFOV) sensors, subtending ~30 arcsec or less. Three of these NFOV sensors (DI, ARDI, and Flash) also image in the visible and near-infrared spectral bands using Si-based CCDs. The 3.6m LWIR sensor, however, acquires NFOV imagery in two thermal-infrared bands simultaneously [3]. Our analysis concentrates on the data gathered during the second AMOS pass, which had the best observing geometry and employed both near-IR and thermal-IR sensors from the largest-available AEOS 3.6m telescope.
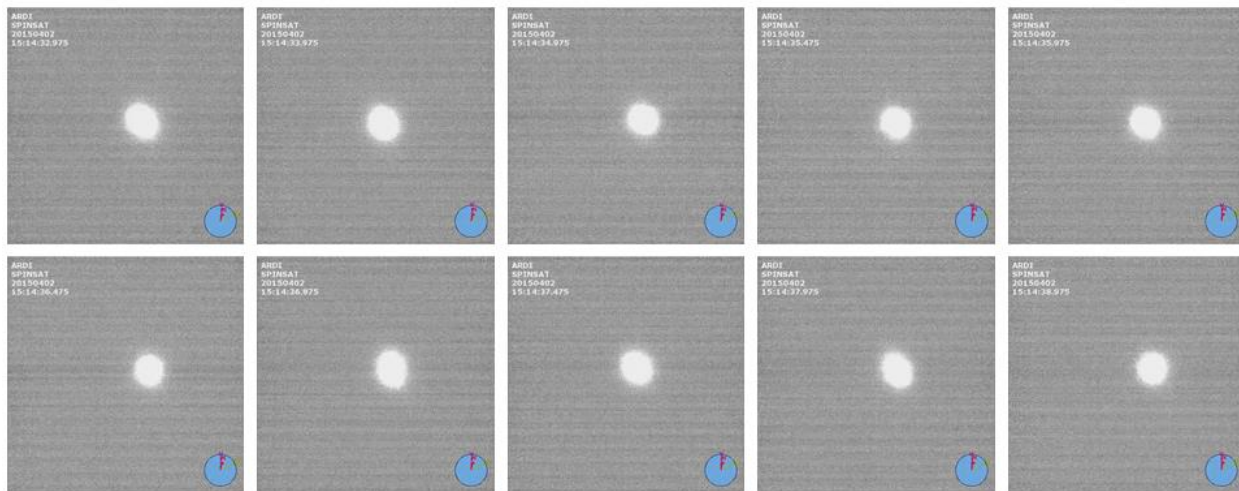

Figure 4. Selected image frames from the AEOS 3.6m telescope's ARDI sensor, spanning the estimated _nominal_ time of one of the commanded SpinSat spin-up/spin-down ESP thruster firings. The frames correspond to the following offset times in seconds relative to the _nominal_ estimate of the 2015-04-02 15:14:36 ESP event: top right to left {-3, -2, -1, -0.5, 0}, bottom right to left {+0.5, +1, +1.5, +2, +3}. No plume-like spatial signature is apparent in any of these images, nor in any of the intervening images.

3.6   Observed Images at or Near the Nominal Times of the Micro-Thruster Firing Events

One of the goals of this campaign of observations entailed characterizing the detectability and spatial/temporal morphology of SpinSat's ESP thruster firings and any associated plumes. Toward this goal, we inspected all images collected from all sensors at or near the estimated _nominal_ times of the thruster-firing events listed in Table 2. Unfortunately, no spatial signatures of the thruster firing events themselves or any associated expanding plumes could be detected, even when the images were subjected to extreme contrast enhancement. Figure 4 illustrates this, showing several frames from the ARDI sensor (collected at a 10 hz frame rate during the second AMOS pass)

bracketing the estimated *nominal* time of the thruster-firing event, 2015-04-02 15:14:36 ± 2 s. No plume-like spatial signature is apparent in any of these images, nor any of the intervening images. Furthermore, similar analysis of all of the other AMOS WFOV and NFOV image data (all subjected to contrast enhancement) also yielded no compelling detections of thruster plumes.

3.7   Observed Light-Curves

Figure 5 shows three light-curve plots acquired by the AEOS telescope's LAAT, ARDI and LWIR sensors during the second AMOS pass. The brightness units are *instrumental magnitudes normalized for range variations*, which provide a logarithmic measure of whole-object brightness, with the effects of object-to-observer range variations removed (but otherwise not radiometrically calibrated). The upper panel (blue) shows data from the LAAT sensor (a 0.6m acquisition telescope co-aligned with the main 3.6m telescope), within the approximate 0.85-1.0 µm spectral range using an 850nm long-pass spectral filter. The middle panel (red) shows data from the ARDI sensor, which is mounted on the 3.6m telescope itself, measuring emissions in the ~0.7-1.0 µm range using an I-band filter; this sensor provided the best signal-to-noise quality data among all of the light-curve data. The bottom panel (green) shows data from one of the two channels of the narrow-field LWIR sensor, also mounted on the 3.6m telescope, measuring thermal emissions in its N2 filter band spanning the ~10-13 µm spectral range [3].
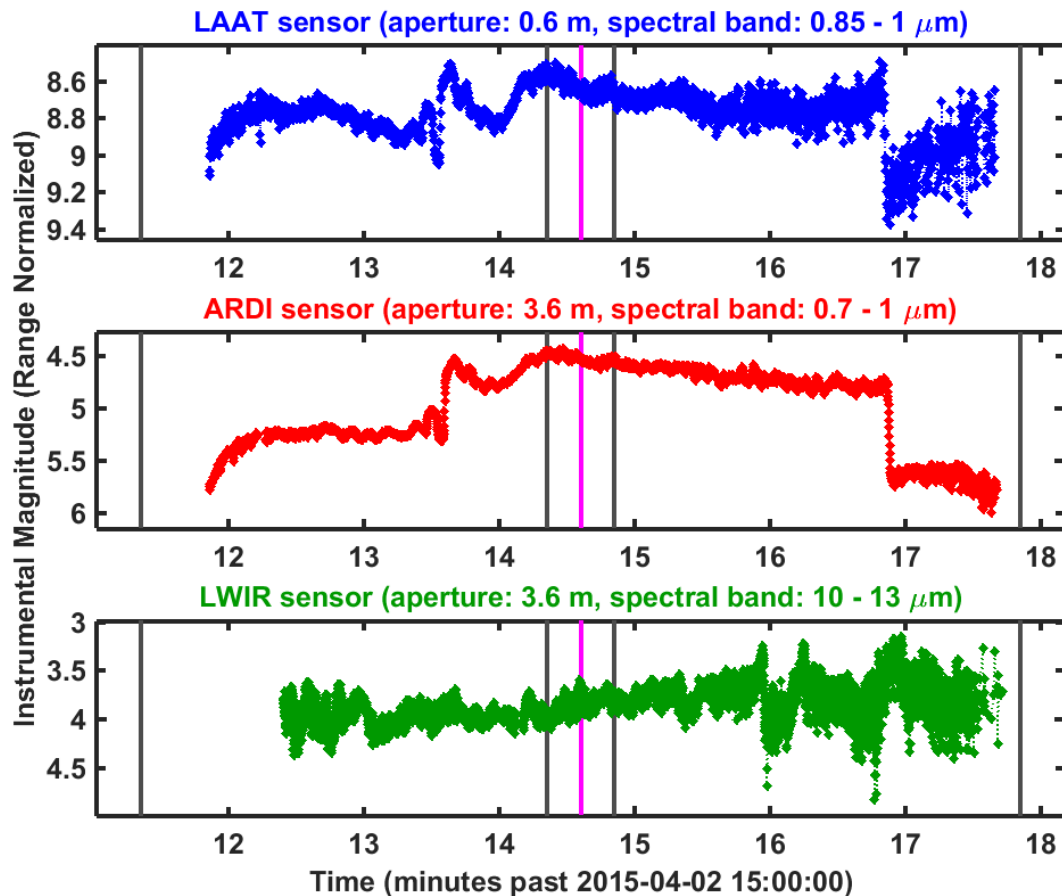

Figure 5. Light-curve plots showing temporal whole-object brightness variations for SpinSat measured during the second observed AMOS pass, using sensors mounted on the AEOS 3.6m telescope. The upper panel (blue) shows wide-field LAAT sensor data, the middle panel (red) shows narrow-field ARDI sensor data, and the bottom panel (green) shows narrow-field LWIR sensor data [3]. The vertical pink lines indicate the estimated *nominal* time of the ESP thruster firing command execution, and the vertical gray lines indicate the estimated *nominal* times of the LED on/off events.
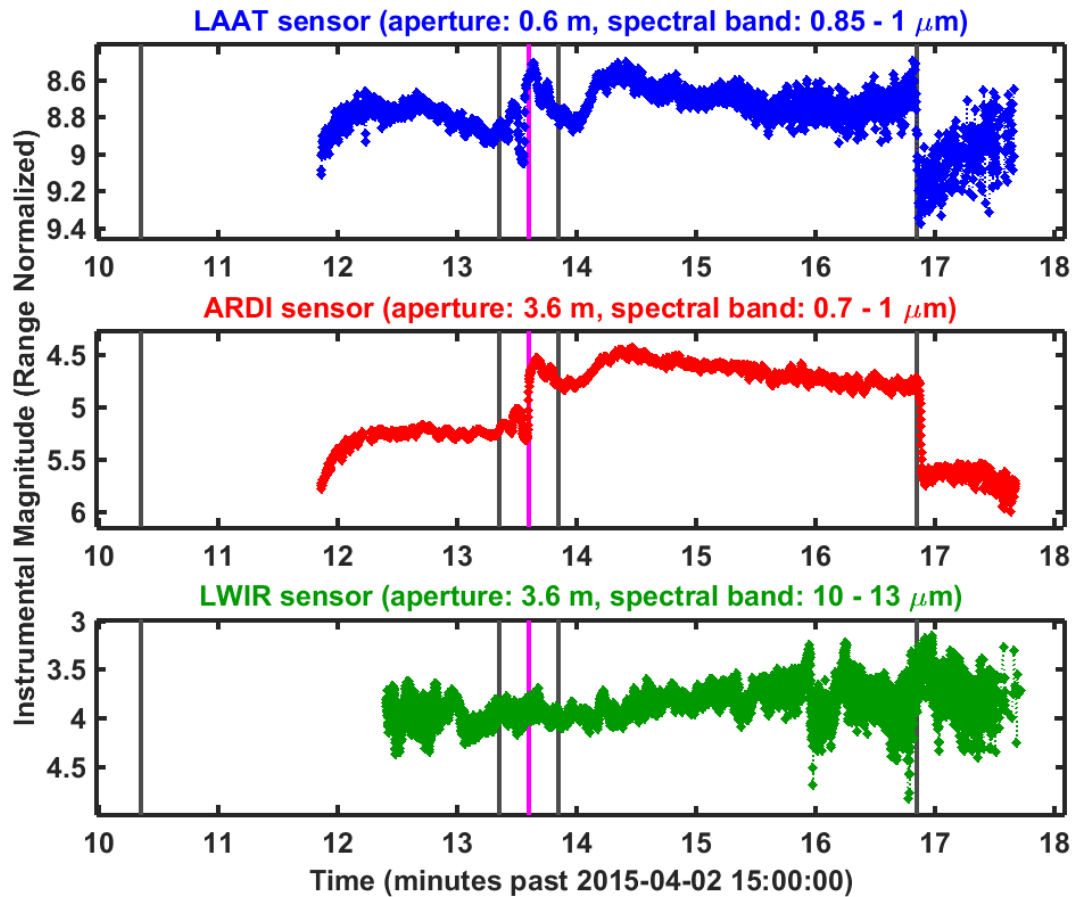
Figure 6. Light-curve plots showing the same data sets as in Figure 5, but now with the vertical pink lines indicating the *1-minute-early* time of the ESP thruster firing command execution, and the vertical gray lines indicating *1-minute-early* times for the LED on/off events.
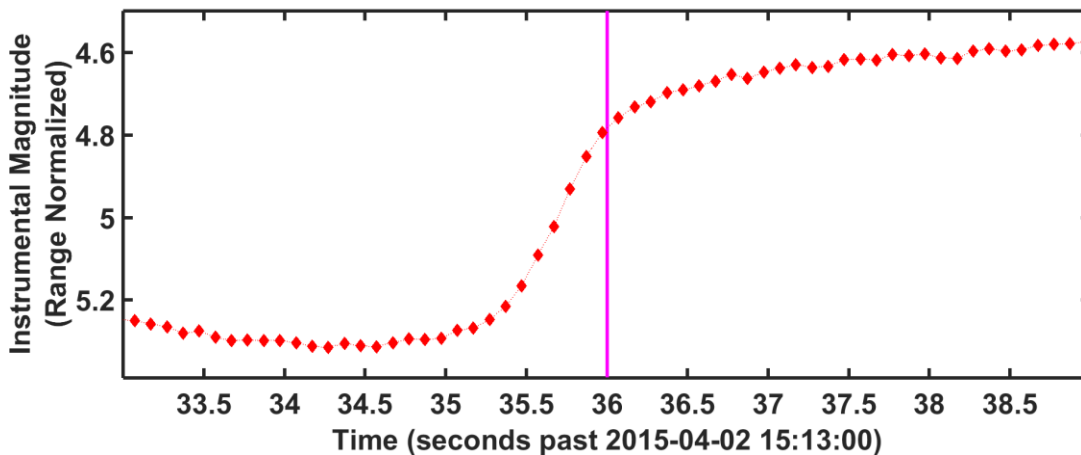

Figure 7. Expanded view of the AEOS 3.6m ARDI sensor light-curve from Figure 6, centered on the time of the sudden increase in near-IR brightness, and closely corresponding to *exactly one minute before the intended ESP thruster firing event* (the pink vertical line). In this *1-minute-early* scenario, the actual thruster firing would have occurred near the beginning of this brightening event, or ~0.5-1.5 s before the *1-minute-early* commanded time, which would falls within the ±2 s uncertainty of the command uplink process.

4   DETECTION OF THRUSTER AND LED EVENTS ONE MINUTE EARLY

The vertical pink lines in Figure 5 indicate the estimated *nominal* times of the ESP thruster firing command execution, and the vertical gray lines indicate the estimated *nominal* times of the LED on/off events (as listed in Table 1). No significant light-curve modulations coincide with these *nominal* event times. This is true for both the near-IR data (plotted in the top two panels) and the thermal emission data (bottom panel). The only notable features in the light-curves are step-like increase in near-IR brightness at ~15:13:36 followed by a step-like decrease in near-IR brightness at ~15:16:52. Although these two light-curve features do not sensibly coincide with any of the *nominal* event times, they do coincide extremely well *if the events had actually occurred one minute earlier than the intended nominal execution times*. Figure 6 shows the light-curves along with these *1-minute-early* event times. In this case, the increase in near-IR brightness at ~15:13:36 closely matches the *1-minute-early* thruster firing, and the sudden dimming at ~15:16:52 closely matches the *1-minute-early* LED deactivation.   This compelling match prompts a hypothesis that an error occurred when entering, calculating or transmitting the event offset times.

4.1   The Likelihood of a *1-Minute-Early* Hypothesis

Such an *exact* one minute error is easily conceivable, possibly created by a typographical error, or a subtraction mistake when calculating relative event times. At this point our team continues to analyze the SpinSat log files to assess the likelihood of this possibility. However, the ground-station operator's current assessment is that this kind of offset would not have been unlikely, in large part because it apparently corresponds to an error of *exactly* one minute, just the kind of round-number error that could occur in the non-automated process. From this point our analysis proceeds based on the assumption that this *1-minute-early* timing actually occurred.

4.2   Light-Curve Signature of *1-Minute-Early* ESP Micro-Thrusters

Figure 7 shows an expanded view of the highest-quality ARDI sensor data near the time of the sudden near-IR brightening event of ~0.5 magnitude (corresponding to an increase in intensity by a factor of ~1.6). This brightening closely coincides with the *1-minute-early* thruster firing time, shown as the pink line. In this case, the ARDI data suggest that the actual thruster firing may have been near the beginning of the brightening event, or about 0.5-1.5 s before the *1-minute-early* command time.
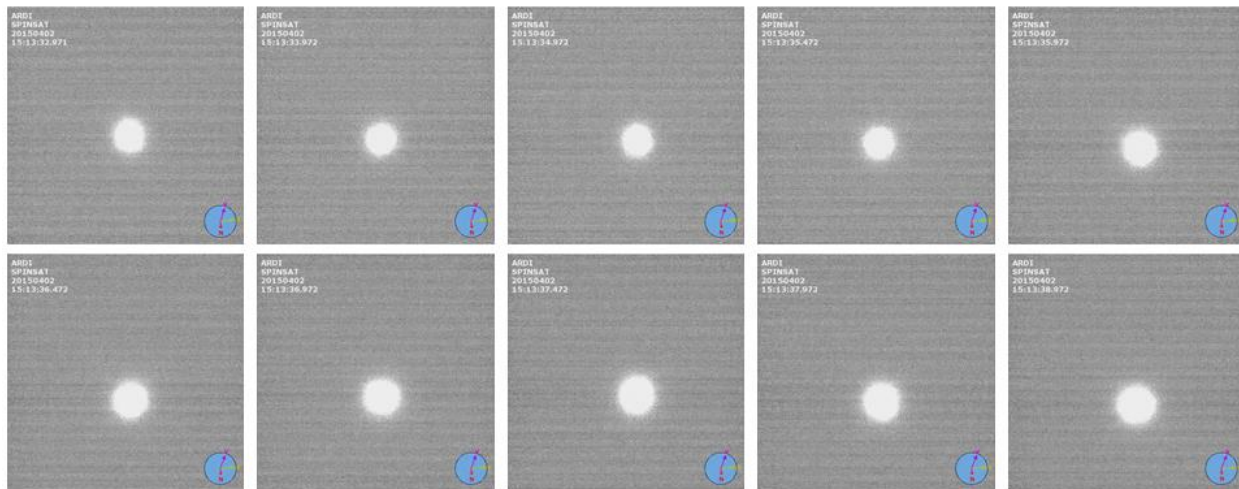

Figure 8. Selected frames from the AEOS 3.6m ARDI sensor, spanning the time period exactly *one minute before* the nominally intended ESP thruster firing. The frames correspond to the following offset times in seconds relative to the *1-minute-early* 2015-04-02 15:13:36 ESP event: top right to left {-3, -2, -1, -0.5, 0}, bottom right to left {+0.5, +1, +1.5, +2, +3}. No plume-like spatial signature is apparent in any of these images, nor in any of the intervening images, but there is a significant increase in overall intensity during this sequence, as can be seen in the growing radius of the bright spot in these contrast-enhanced images.

4.3   Search for the Spatial Signature of *1-Minute-Early* ESP Micro-Thruster Plumes

Figure 8 shows ARDI sensor images within a few seconds of the observed light-curve brightening, which again would closely coincide with a hypothesized *1-minute-early* thruster firing. Once again, no spatial signatures of the thruster events themselves or any associated expanding plumes could be detected (even when the images were subjected to extreme contrast enhancement). There is an apparent increase in overall intensity during this image

sequence, as revealed by the growing radius of the bright spot in these contrast-enhanced images. This means that the thruster effects causing the overall brightening remain unresolved or below the noise detection threshold.

4.4   Light-Curve Signature of *1-Minute-Early* LED Deactivation Event

The near-IR dimming event at ~15:16:52 in Figure 6 closely corresponds to a *1-minute-early* LED deactivation command. This ~0.8 magnitude dimming corresponds to a decrease of ~50% or more in intensity, and lasts less than about two seconds. If this is indeed the signature of the LEDs being turned off, it begs the following two questions: 1) Why isn't a comparable brightening observed 3.0 m earlier, at the time of the previous LED-on command? and 2) Why isn't a similar dimming observed 3.5 m earlier, at the time of the previous LED-off command? These two questions can be explained by the fact that a separate set measurements (discussed below) indicate that SpinSat was rotating relatively slowly at the time of these observations and that the meridian-line of LEDs could have been oriented largely away from the AMOS sensors during these two preceding events. Notably, the near-IR light-curves in Figure 6 do show a ~0.6 magnitude brightening trend starting ~10 s after the post-thruster LED activation, and lasting ~30 s. Preliminary analysis indicates that this trend is consistent with the already activated LEDs rotating into view of the sensors. Subsequently, the LEDs could have remained in sufficient view to cause the sudden dimming observed at ~15:16:52 which occurred ~1 s after the *1-minute-early* LED-off command.

5   SPINSAT ROTATION RATE FROM SATELLITE LASER RANGING OBSERVATIONS

Separate observations using Satellite Laser Ranging (SLR) returns from the SpinSat's retro-reflectors [1] indicate that during the AMOS passes the satellite had a rotation rate of about 1.0-1.7 deg/s, corresponding to a rotation period of roughly 3.5 to 6 minutes. This relatively slow rotation indicates that SpinSat may have only executed one or perhaps two complete rotations during the period spanned by the light-curves shown in Figure 6. This confirms the idea discussed previously that some of the LED on/off events may not have been fully detected, simply because the meridian-line of LEDs was rotated to be oriented largely on the opposite side of SpinSat than the sensor. It also explains why the light-curve data do not show a periodicity pattern expected from a rapidly rotating object.

6   CONCLUSIONS AND FUTURE WORK

The AMOS observations of SpinSat suggest that a timing error of exactly one minute likely occurred during the command-load uplink process. Otherwise the features of the AMOS light-curve data are difficult to explain. Based on this *1-minute-early* assumption the following conclusions can be drawn from the data collected on 2015-04-02 and shown in Figures 6, 7 and 8:

1. The ESP micro-thruster firing at ~15:13:36 caused a sudden near-IR brightening of ~0.5 magnitude.
2. The spatial signature of ESP micro-thrusters and/or their associated plumes were not detectable in the contrast-enhanced imagery from the narrow- and wide-field imaging sensors on the AEOS 3.6m telescope.
3. The ESP thruster or LED on/off events were not detected in the thermal-IR imagery or the thermal-IR whole-object radiometry using the AEOS 3.6m telescope LWIR instrument.
4. The LED deactivation at ~15:16:51 caused a sudden near-IR dimming of ~0.8 magnitude.
5. The preceding LED activation and deactivation events did not create comparable sudden brightness changes because, at the time of these command executions, the line of LEDs was likely oriented largely on the opposite side of the sphere than the AMOS sensors.

The second and third of these conclusions deserve further discussion. Solid propellant thrusters much larger than those on SpinSat are known to create plumes observable from ground-based sensors. Our study indicates that plumes from SpinSat's tiny ESP thrusters are difficult to detect in near-IR imagery, as well as in thermal-IR imagery or radiometry, even using the high-quality sensors mounted on the large AEOS 3.6 m diameter aperture telescope. Notably, many new small satellites such as CubeSats are increasingly likely to employ these kinds of thrusters in the future. Fortunately, our analysis of the AMOS SpinSat observations suggests that such CubeSat-class micro-thrusters can be detected using broad-band near-IR radiometry.

7   REFERENCES

1. Nicholas, A., et al., "SpinSat Mission Overview", Proceedings of the 2013 AIAA/USU Conference on Small Satellites, Advanced Tech. Session, SSC13-I-3, http://digitalcommons.usu.edu/smallsat/2013/all2013/46
2. Pinto, O., et al., "The South Atlantic Magnetic Anomaly: Three Decades of Research", J. Atmos. Terr. Phys., **51**, 251-365, 1992.
3. Witte, D., "The AEOS LWIR Imager: A Tool for Space Object Thermometry," *The 1999 AMOS Technical Conference Proceedings*, Kihei, HI, 1999.